Controlling orientation, polymorphism, and crystallinity in thin films of poly(lactic-acid) homopolymer and stereocomplex aligned by high temperature rubbing

Marion Brosset, Laurent Herrmann, Céline Kiefer, Thierry Falher, Martin Brinkmann

Controlling orientation, polymorphism and crystallinity in thin films of poly(lactic-acid) homopolymer and stereocomplex aligned by high temperature rubbing

Marion Brosset[1,2], Laurent Herrmann[1], Céline Kiefer[3], Thierry Falher [2], Martin Brinkmann[1*]

1 Université de Strasbourg, CNRS, ICS UPR 22, F-67000 Strasbourg, France,

2 IPC – Pôle Universitaire d'Alençon, Campus de Damigny, 61250 Damigny - France

3 Université de Strasbourg, IPCMS, UMR 7504, F-67000 Strasbourg, France

* e-mail : martin.brinkmann@ics-cnrs.unistra.fr

Abstract

High temperature rubbing is a fast and low-cost method that can align semi-crystalline polymers such as poly(lactic acid) (PLA) by application of a shear-force via a rotating cylinder covered with a microfiber cloth on a thin film maintained at high temperature. A multi technique approach uncovers the role of rubbing temperature and film thickness on the PLA thin film structure. Both poly(L-lactic acid) (PLLA) and the stereo-complex (SC-PLA) can be readily aligned by high temperature rubbing. The rubbing temperature T_R and the film thickness are the key parameters that control polymorphism, in-plane orientation, crystallinity and contact plane of the polymer crystals. Rubbing PLLA films in the range 80°C-140°C affords different aligned polymorphs (mesophase, α', α'+α mixtures and pure α phase) depending on the rubbing temperature. Pure α form of PLLA with 53% crystallinity is obtained at T_R=140°C whereas pure oriented crystalline SC-PLA films are obtained by rubbing at 200°C.

Keywords. Bio-sourced polymer, crystallization, structure

I. Introduction.

Poly(lactic acid) (PLA) is a commodity bio-sourced polymer that has been widely investigated and used for various applications including packaging and medical use.[1-3] This polymer is also biodegradable and can therefore be considered as an alternative polymer for packaging materials to replace classical fuel-based synthetic polymers.[4,5] For the majority of applications using PLA, the crystallinity of this polymer plays a key role in particular for optical, mechanical and barrier properties.[6] On one side, the structure of PLA is related to its polymorphism that has been thoroughly investigated. PLLA can form at least four polymorphs: i) the stable α form made of 10_3 helices organized in an orthorhombic unit cell, ii) the pseudo-hexagonal α' structure that is a disordered form of the α structure, iii) the β form made of 3_1 helices obtained under strong shear conditions and iv) the γ form (10_3 helices) grown by epitaxy.[7,8] The disorder in the α' form has been described as a statistical disorder of "up" and "down" stems. [8] Due to the presence of an asymmetric carbon center in the chain of PLA, two enantiomers of PLA can be formed: poly(L-lactide) (PLLA) and poly(D-lactide) (PDLA). Equimolar blends of PLLA and PDLA form a stereocomplex (SC PLA) that can crystallize in a trigonal unit cell and has a high melting temperature of 220°C. [9-11]

Like most semi-crystalline polymers, the physical and mechanical properties of PLA depend strongly on the polymorphism, crystallinity and morphology that are determined by the chosen processing conditions.[6] Different means such as alignment by hot drawing, biaxial drawing or addition of nucleating agents have been used to improve the properties of PLA thin films. The crystallinity of PLLA is improved by addition of nucleating agents such as clay, talc or N-N'-N''-tricyclohexyl-1,3,5-benzene-tricarboxylamide.[12-14] However, such additives may be prohibited for certain applications of PLLA, especially in the case of food packaging as they may migrate out of the thin films in time. Orientation by hot drawing of PLA is a well-established method to tune the crystallinity of PLA.[15-18] Recently, very highly oriented PLLA

thin films (thickness below 50 nm) were produced by the melt-draw technique introduced by Petermann et al. [17,18] The application of shear stress can help generate oriented bundles of chains that act as nucleating seeds to direct the growth of PLA lamellae. When both shearing and high pressure are used at a given temperature, specific structural features and polymorphs can be generated. For instance, drawing PLLA at 80°C leads to a metastable mesophase that undergoes cold crystallization to the α' form at T>90°C. The pure β form PLLA can be produced by melt-crystallization for a shear of 13.6 s^{-1}, pressure of 100 MPa and crystallization temperature of 160°C.[19] The relation between polymorphism and certain properties such as Young modulus and gas permeability of PLA was also demonstrated, highlighting the importance of a structural control of PLA.[6]

In this contribution, we investigate the structure and orientation in PLA thin films (14-150 nm) aligned by high temperature rubbing. This method consists in applying a rotating cylinder covered with a microfiber cloth onto a thin film of PLA maintained at elevated and controlled temperature during rubbing (T_R). It has been widely used to orient polymer semiconductors such as regioregular poly(3-hexylthiophene) (P3HT), other low bandgap polymers as well as bisphenol A polycarbonate and hybrid materials made of polymers and CdSe nanorods.[20-24] As a general trend, the alignment can be substantially improved when the temperature of the films increases and approaches the melting temperature of the polymer. As an example, rubbing P3HT at 240°C affords highly oriented thin films with an in-plane order parameter of 0.85 and crystallinity of 60%. [22] So far, high-T rubbing has never been used for biosourced polymers and it is therefore important to probe the efficacy of this method for this important class of polymers. Alignment and crystallization control of thin PLA films can be of interest for numerous applications including packaging but also the fabrication of piezoelectric PLLA layers or alignment layers for other molecular or polymeric systems. [25,26]

II. Experimental section.

a) Materials

The macromolecular parameters of all polymer samples used in this study are collected in Table S1. They are obtained by Size Exclusion Chromatography (Shimadzu LC-2OAD, DGU 20A, SIL-20AHT, CTO-10AC VP at 30°C and 3 PLGelB columns and two detectors UV Shimadzu SPD-10A and RID-10A) in chloroform with PS calibration. Pure Poly(L-lactide) and Poly(D-lactide) were purchased from Total Corbion whereas PLA-2%D (4032D) was purchased from NatureWorks. Sodium Poly(styrenesulfonate) (NaPSS) was purchased from Sigma Aldrich.

b) *Thin films preparation and orientation.*

The preparation of oriented poly(lactic-acid) films by high-temperature mechanical rubbing follows the procedure described in previous publications. PLA is deposited on a sacrificial layer of NaPSS on glass slides. NaPSS films are formed by spin-coating a solution (10 mg/ml in water) at 3000 rpm for 60 s on clean glass slides (cleaned by ultrasonication for 15 min successively in acetone, ethanol, aqueous solution of Hellmanex and three times in distilled water). The PLA films are deposited on NaPSS/glass by doctor blading. The film thickness is controlled by adjusting the concentration of the polymer solution in the range 5 - 20 mg/ml in chloroform at 50 °C. For this range of concentrations, the obtained PLLA films have a thickness that increases from 14 nm to 150 nm (Figure S1). Prior to rubbing, the films are melted at T=200°C and quenched in ice water to obtain amorphous PLA films. This is possible for PLA because it is a very slow-crystallizing polymer.[8] Figure S2 shows the ED pattern of the PLLA quenched film in an amorphous state showing no diffraction peaks versus the film after thermal annealing for 10 min at 165°C showing characteristic Scherrer rings typical of the α form. The use of amorphous PLA films is important as there are no pre-existing crystals in the films before rubbing and the entire film can be aligned and crystallized during

the rubbing of the films. For the alignment of the films, a homemade rubbing machine is used. It is composed of a rotating cylinder (4 cm diameter) covered by a microfiber cloth (non-woven polyester cloth). The rubbing is performed by applying the rotating cylinder (600 RPM) with a pressure of ca. 2-3 bar on the translating sample holder (1 cm/s). Pressure control is via a pneumatic system controlling the application of the film The sample holder consists of a translating heating stage that can be heated to a given rubbing temperature (T_R). The PLA film on the glass substrate is placed on the heating stage and the sample's temperature is allowed to equilibrate at T_R for 10 seconds before rubbing. Prolongated thermal annealing of the PLA film at T_R on the hot stage of the rubbing machine (> 1 min) prior to rubbing is detrimental for the film alignment as it promotes crystallization of non-oriented spherullites. A rubbing cycle is characterized by the so-called rubbing length, i.e., the length of the rubbing tissue applied on a given point of the sample. In the present case, it is 50 cm.

c) Structural Analysis, differential scanning calorimetry and FTIR spectroscopy.

Transmission Electron Microscopy. For TEM analysis, the oriented areas were identified using polarized optical microscopy (Leica DMR-X microscope). The polymer films are coated with a thin amorphous carbon film and removed from the glass substrate by floating on a distilled water and subsequent recovery on TEM copper grids. TEM was performed in low dose bright field and diffraction modes using a CM12 Philips microscope equipped with a MVIII (Soft Imaging System) camera. To observe the lamellar structure in bright field TEM with sufficient contrast, thin films prepared from 5mg/ml PLLA solution were used. Calibration of the reticular distances in the Electron Diffraction (ED) patterns is made with an oriented PTFE film. Beam exposure is set to a minimum using the low dose system to avoid damaging the film under the electron beam.

Herman's order parameters f_H were extracted from the ED patterns using ImageJ software. The values of f_H are an average of 4-5 ED patterns for each rubbing temperature.

Electron diffraction patterns were calculated using the Cerius2 software with the published structures for the α form and PLA SC.[8]

Differential Scanning Calorimetry (DSC). DSC experiments were performed on a TA Instruments DSC Q200. 8-10 films (*ca*. 3 mg) were removed from their glass substrate by floating on distilled water and recovered on an aluminum DSC pan. One heating and one cooling steps in a temperature range from 40°C to 210°C were used to characterize the films after alignment by rubbing (10 °C/min).

Fourier transform infrared (FTIR) spectroscopy. FTIR was performed using Perkin Elmer Spectrum Two spectrophotometer in transmission mode. The PLA samples were transferred by floating on distilled water to Si(100) substrates (Silchem). The spectra were recorded in the 400-4000 cm^{-1} spectral range, with a resolution of 4 cm^{-1}. An average spectrum of 16 scans was recorded for each sample.

III. Results and discussion.

1. Orientation of PLLA by high-T rubbing.

a) Impact of rubbing temperature on thin film polymorphism of PLLA.

Differential Scanning Calorimetry has been used to follow the structure of the rubbed PLA thin films (Pure PLLA and PLA with 2% D stereo-defects) as a function of the rubbing temperature T_R. Of interest is the first heating scan since it helps visualize potential re-crystallization processes in the rubbed thin films and the existence of polymorphism. In particular, as for rubbed P3HT, DSC can evidence the presence of an oriented mesophase in the rubbed thin films that is characterized by a cold crystallization exotherm in DSC.[27,28]

Figure 1.a exemplifies the evolution of the DSC trace *versus* rubbing temperature T_R for pure rubbed PLLA films. Alignment of PLLA was only observed for rubbing temperatures above the glass transition temperature T_g, underlining the importance of the rubbing temperature for PLLA films. Films rubbed at 80°C show two exotherms, a broad one centred

at 85-90°C and a second weak one right before the melting endotherm. The first exotherm is attributed to the transformation of an oriented mesophase into the oriented α' form of PLLA, in line with reports on PLLA films drawn at a temperature slightly above T_g. [29] For T_R=100°C, the first exotherm seen for T_R=80°C is almost fully suppressed. No mesophase is formed for T_R=100°C, the rubbed films are in α' form, as confirmed by TEM electron diffraction. The second exotherm is observed for both T_R=80°C and 100°C and centered at 155°C-160°C. It is followed by a single melting endotherm centered at 174-175°C. In agreement with earlier reports, this exotherm is attributed to a melting-recrystallization process of the α' form into the α form.[6]

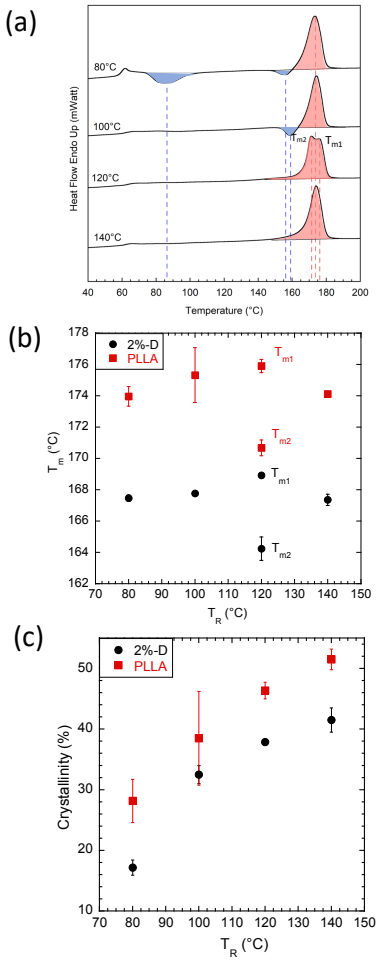

Figure 1. a) DSC trace upon first heating cycle of the rubbed PLLA thin films as a function of increasing rubbing temperature. The exotherms are highlighted in blue whereas the

melting endotherms are shown in red. (b) Observed melting temperatures (T_m) of rubbed PLLA thin films (pure PLLA and with 2% D stereo defects) as function of the rubbing temperature (T_R). Note that for T_R=120°C, two melting endotherms are observed with melting temperatures T_{m1} and T_{m2}. c) Evolution of the crystallinity extracted from the melting enthalpies of rubbed PLA thin films (pure and with 2% D stereodefects).

For $T_R \geq 120$°C, no more exotherm is observed but two clear melting endotherms are visible for T_R=120°C at T_{m1}=174°C and T_{m2}=170.5°C (Figure 1.b). Similar observations were made for non-oriented PLLA thin films crystallized close to 120°C.[29] Due to the polymorphism of PLLA with two structurally similar α' and α phases, both growth rates and lamellar thicknesses show an anomalous behaviour in the range 100- 120°C.[6,8] 120°C corresponds to the temperature for which the growth rates of both α' and α forms of PLLA are almost equal. Accordingly, upon rubbing at 120°C, both oriented crystals of α and α' forms are generated upon rubbing. Crystals of α' form undergo melt-crystallization to the α form when approaching the melting temperature of the α form. Therefore, the two melting endotherms evidenced by DSC in the films rubbed at 120°C are attributed to i) α crystals formed by melting/recrystallization of the α' phase and to ii) α crystals formed directly by rubbing at 120°C. Hence, rubbed PLLA films at 120°C consist of a mixture of oriented α' and α crystals. For T_R=140°C, only one melting exotherm and no exotherm are observed, indicating that the films consist of oriented α crystals only (in agreement with the results of electron diffraction) generated by rubbing at 140°C.

The same DSC experiments were also performed for the PLA sample with 2% D stereodefects (PLA-2%D). The observed trends are similar to those evidenced for pure PLLA (see Figure S3). The main difference is related to the film crystallinity. Expectedly,

the crystallinity in rubbed PLA-2%D is lower than that for the pure PLLA polymer (Figure 1.c). As an example, for T_R=140°C χ=53% for pure PLLA *versus* χ =44% for PLA-2%D.

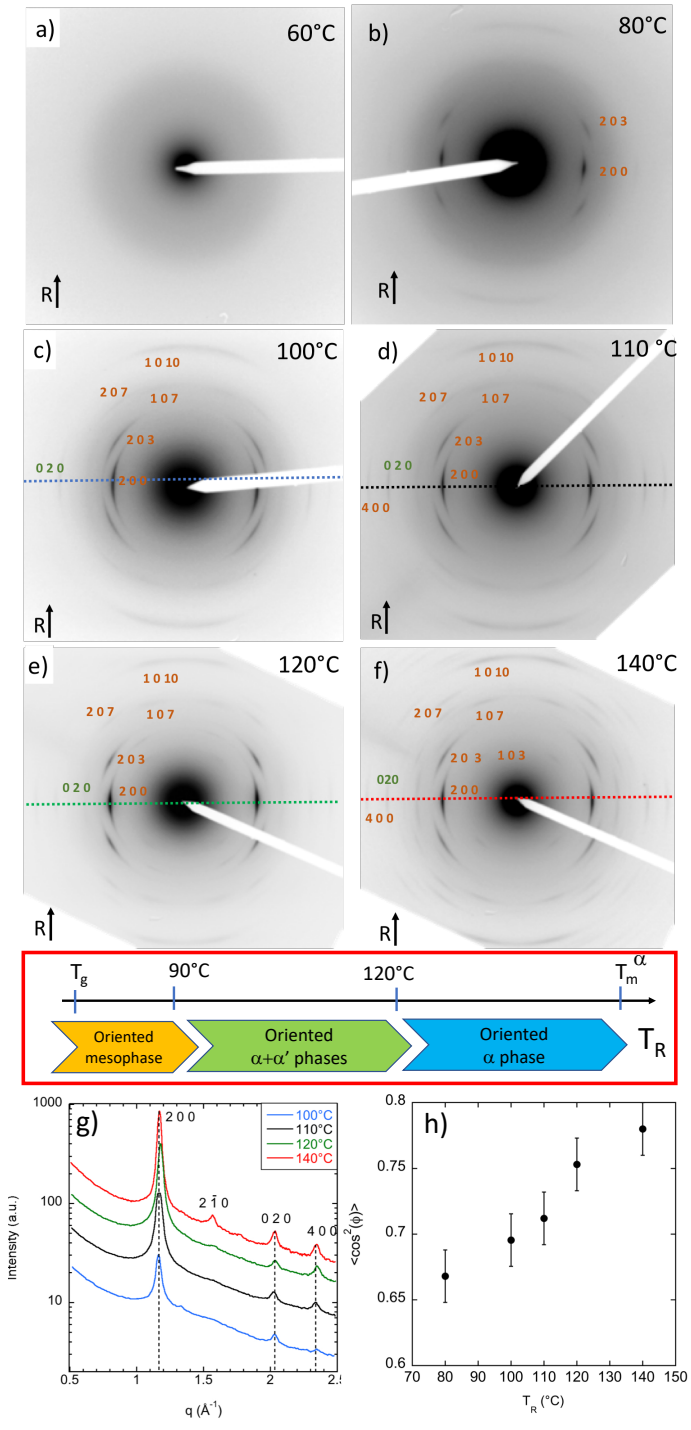

Figure 2. a)-f) Evolution of the electron diffraction pattern of PLLA rubbed films as a function of rubbing temperature T_R in the range 60°C-140°C The rubbing direction (R) is vertical. The main reflections have been indexed using the α form of PLLA. g) Evolution of the equatorial

section profile of the ED pattern as a function of T_R. For clarity the profiles are shifted along the ordinate axis. h) Evolution of Herman's orientation parameter f_H as a function of the rubbing temperature T_R for rubbed PLLA thin films.

The highest crystallinity obtained in the present case is quite close to the 55% value reported by Li et al. for melt-drawn PLLA thin films.[16] Two melting endotherms at T_{m1} and T_{m2} are also observed for PLA-2%D films rubbed at 120°C. The observed melting temperatures T_{m1} and T_{m2} for PLA-2%D are below the ones obtained for pure PLLA, which is consistent with earlier reports on the dependence of polymorphism on the percentage of stereodefects.[7]

The rubbing temperature can affect several aspects of the thin film structure such as polymorphism, crystal dimensions and crystallinity as well as in-plane orientation and contact plane of the crystals.[21,22] For instance, in rubbed P3HT films, T_R controls the contact plane of the crystals that change from face-on to edge-on with increasing T_R. The in-plane orientation is also determined by T_R. The general trend is of a higher in-plane alignment of crystals when T_R approaches the melting temperature.

Electron diffraction is a valuable method to follow those structural changes in the rubbed thin films of PLLA as a function of increasing T_R. Figure 2 shows the typical evolution of the ED pattern of rubbed PLLA with T_R from 60°C to 140°C. Films rubbed at a temperature close to T_g are not oriented and do not show any structuring. All PLLA films rubbed at $T_R \geq 80$°C show some in-plane orientation. For $80° \leq T_R \leq 100$°C, the ED pattern contains only a limited number of rather broad reflections that are reminiscent of the α' phase.[6] For T_R=120°C, the reflections sharpen and new ones start to appear, indicative of the formation of α crystals. The α form is identified by the presence of well-defined (1 0 ℓ) reflections with ℓ =3,7,10 that are absent when $T_R \leq 110$°C. In agreement with DSC data, the films rubbed at 120°C consist very likely of both α and α' crystals. Finally, for T_R=140°C, the diffraction pattern becomes

remarkably well defined with numerous reflections that unambiguously identify the α form of PLLA.[8]

The polymorphism was also investigated by FTIR spectroscopy since the mesophase, the α' and α polymorphs of PLLA have typical signatures (Figure 3). For instance, the α form is characterized by a typical band located at 921 cm^{-1}.[29,30] This band has been attributed to the coupling of C—C backbone stretching with the CH_3 rocking mode, for a 10_3 chain conformation of PLLA observed for both α and α′ PLLA.[30,31] In Figure 3, this band shows a clear jump in intensity between T_R=90°C and T_R=100°C. In the same temperature range, a characteristic change in the FTIR spectrum is observed in the 1320-1240 cm^{-1} range: i) the decrease of the $\delta_{(CH)} + \nu_{(COC)}$ (1268-1272 cm^{-1}) band attributed to the mesophase and ii) the increase of the intensity of the $\delta_{2(CH)}$ band (1294-1300cm^{-1}) corresponding to crystalline PLLA. The narrowing of the 871 cm^{-1} band (corresponding to a $\nu_{C\text{-}COO}$) is consistent with the increased crystallinity observed by DSC with increasing T_R. Importantly, the 912 cm^{-1} band characteristic of β-form PLLA is absent in the rubbed thin films.[30,31] Overall, these results show that for $T_R \leq 90$°C, the chain conformation is possibly more disordered than in the α' phase and that the films have a structure more alike the structure of a drawn mesophase, supporting the results obtained by DSC. [27,28]

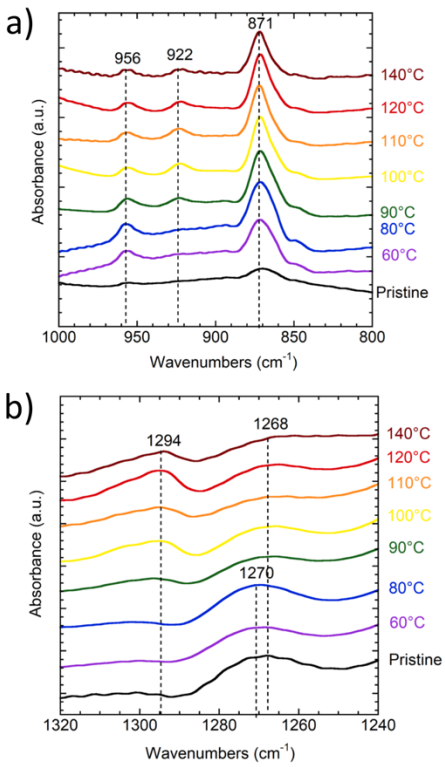

Figure 3. Evolution of the polymorphism in rubbed PLLA thin films as a function of the rubbing temperature (T_R) for the 800-1000 cm^{-1} range corresponding to skeletal stretching and CH_3 rocking (a) and the 1240-1320 cm^{-1} range corresponding to CH bending and C-O-C stretching (b). For comparison the spectra of the amorphous non-rubbed film are shown. For clarity, the spectra were normalized in intensity and shifted along the ordinate axis.

b) Impact of rubbing temperature on in-plane orientation and film morphology of PLLA.

Beside crystallinity, the rubbing temperature can impact the in-plane orientation of the PLLA chains. As observed in previous studies on polymers such as P3HT, the increase of T_R can substantially improve in-plane orientation and crystallinity. While DSC has shown that the crystallinity χ of pure PLLA and PLA-2%D is indeed improved with T_R, it is necessary to verify how T_R impacts the in-plane orientation of the PLLA films. The evolution of the in-plane

orientation of PLLA crystals is quantified by using Herman's orientation factor f_H that can be calculated for the equatorial 2 0 0 reflection (for a random in-plane distribution of crystals f_H=0, whereas for a perfect in-plane alignment of all PLLA crystals f_H=1). f_H has been calculated using the following equations[19,32]:

$$f_H = \frac{3\langle cos^2\varphi\rangle - 1}{2} \quad (1)$$

$$\langle cos^2\varphi\rangle = \frac{\int_0^{\pi/2} I(\varphi) cos^2\varphi sin\varphi d\varphi}{\int_0^{\pi/2} I(\varphi) sin\varphi d\varphi} \quad (2)$$

where φ is the azimuthal angle between the rubbing direction (R) and the azimuthal direction along the intensity profile of the 2 0 0 reflection.

As seen in Figure 2.f, Herman's orientation parameter f_H increases from 0.66 to 0.78 when T_R increases from 80°C to 140°C. The final value of the order parameter is close to that obtained from UV-vis spectroscopy in oriented P3HT films rubbed right below the melting temperature. It is however lower than f_H=0.99 found for PLLA tapes oriented by drawing at 130°C with a drawing ratio of 8. [33] We anticipate that increasing the rubbing length or the pressure during rubbing might lead to a better alignment of the PLLA films. We do not observe that the polymorphism in the rubbed PLLA films coincides with a clear-cut discontinuity in the alignment level of the PLLA films. Polymorphism is accordingly essentially driven by the rubbing temperature that corresponds to the crystallization temperature and not to the alignment of polymer chains.

Finally, the morphology of the thin films was followed as a function of the rubbing temperature by POM and TEM in bright field mode. Polarized Optical Microscopy (POM) shows that the films rubbed at $T_R \leq 90$°C are poorly birefringent whereas for $T_R \geq 100$°C, a stronger

birefringence sets in (see Figure 4). The best alignment is indeed observed for T_R=140°C. However, at such high temperatures, the rubbing process induces pin holes in the thin films that could be detrimental for applications such as barrier properties. As seen in Figure 4, no regular lamellar morphology could be observed at T_R=100°C. The FFT of the bright field images indicate no well-defined lamellar periodicity. Only a loose assembly of lamellae with an overall low density can be seen suggesting that the nucleation induced by rubbing is not sufficiently dense to ensure a uniform coverage of the film surface with crystalline lamellae. For $T_R \geq 120$°C, a regular array of crystalline lamellae is observed with a very well-defined periodicity (see FFT in Figure 4). The lamellar periodicity is in the 23 nm - 28 nm range.

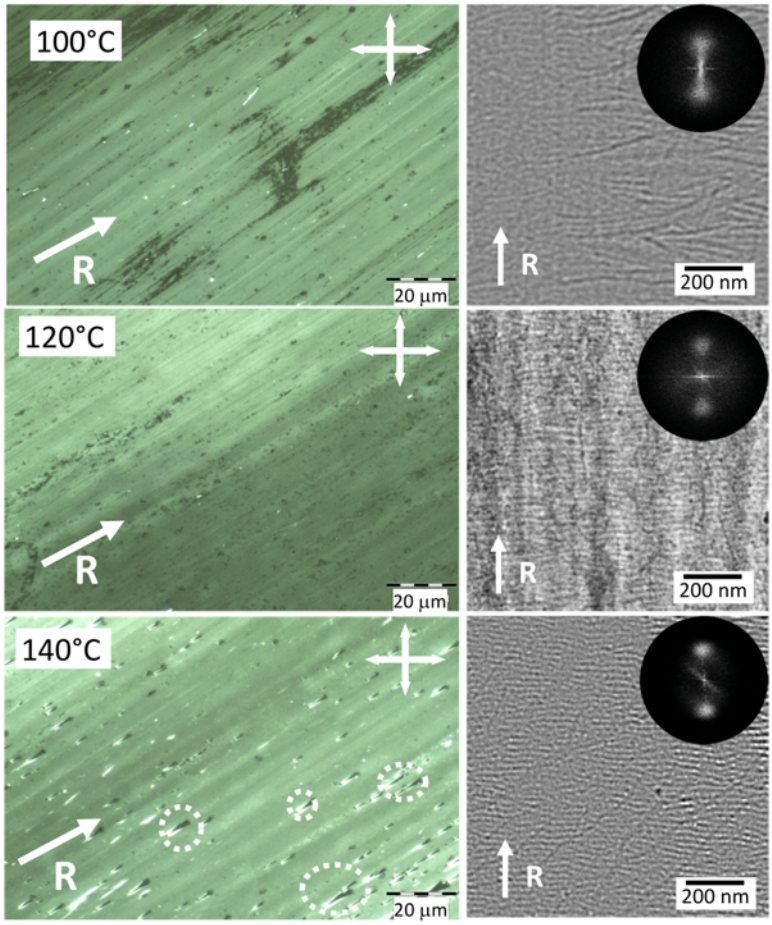

Figure 4. Evolution of the morphology in PLLA thin films oriented by high-T rubbing at different temperatures as observed in Polarized Optical Microscopy (under crossed polarizers) (left) and TEM Bright Field (right). R is the rubbing direction. For T_R=140°C, pinholes are

highlighted by dotted circles in the POM image. The Fast Fourier Transform of the BF images is shown as an inset for each rubbing temperature.

c) Influence of film thickness on crystal contact plane of PLLA.

When dealing with thin films of thickness close to the lamellar thickness, it is essential to verify if the film thickness or the rubbing temperature influence the contact plane of PLLA crystals. Referring again to P3HT, the rubbing temperature is known to influence the contact plane of oriented lamellae from dominant (010) at low T_R to (100) at higher T_R.

In particular, we demonstrate that the initial film thickness has an important influence on the majority contact plane of the crystals. The film thickness was tuned by controlling the PLLA concentration in $CHCl_3$ used for doctor blading the films. In Figure 5, we compare the ED patterns of PLLA films rubbed at 100, 120 and 140°C for thicknesses of 14 nm and 150 nm. The calculated ED patterns for α PLLA crystals are also shown in Figure 5.e and 5.f for the [100] and the [010] zone axes. For all T_R, the reflections in the ED patterns of the very thin films differ from the thick film ones. For instance, the 0 2 0 equatorial reflection is stronger than the 2 0 0 for the 14 nm-thick films when compared to the 150nm-thick films (see section profile in Figure S4). The indexation of the dominant reflections according to the α structure indicates that the 14nm-thick films are made of crystals with a dominant (100) contact plane whereas the 150nm-thick films are made of a majority of crystals with (010) contact plane. This is an original finding. It shows that the orientation of PLLA crystals in very thin films (15 nm i.e. less than the lamellar periodicity) can differ from the dominant orientation found in thicker thin films. This result may be related to the orientation of the fast growth direction of PLLA crystals with respect to the substrate normal. It has been reported that for spherullitic growth at T>110°C, the **a**-axis is the fast growth direction whereas for a temperature of crystallization below this temperature it is the **b**-axis.[8] Our results show that the change in apparent contact

plane depends on the film thickness in rubbed PLLA films but not on TR: it is observed for 100°C and for 140°C. Our interpretation is accordingly different. We propose that the preferential contact plane in 14nm-thick PLLA films is enforced by rubbing at the free surface of the film that is in contact with the microfiber cloth. This preferential contact plane is progressively lost when crystallization propagates in the bulk of the thicker 150nm PLLA films, resulting in a fiber-like structure of the films. Similar preferential contact planes of polymer crystals were observed in other rubbed polymer films. Most illustrative examples are provided by rubbed bisphenol A polycarbonate films crystallized from acetone vapor and rubbed P3HT films ($T_R \leq 100°C$). These observations suggest that this phenomenon is more general and not limited to PLLA. [22,34]

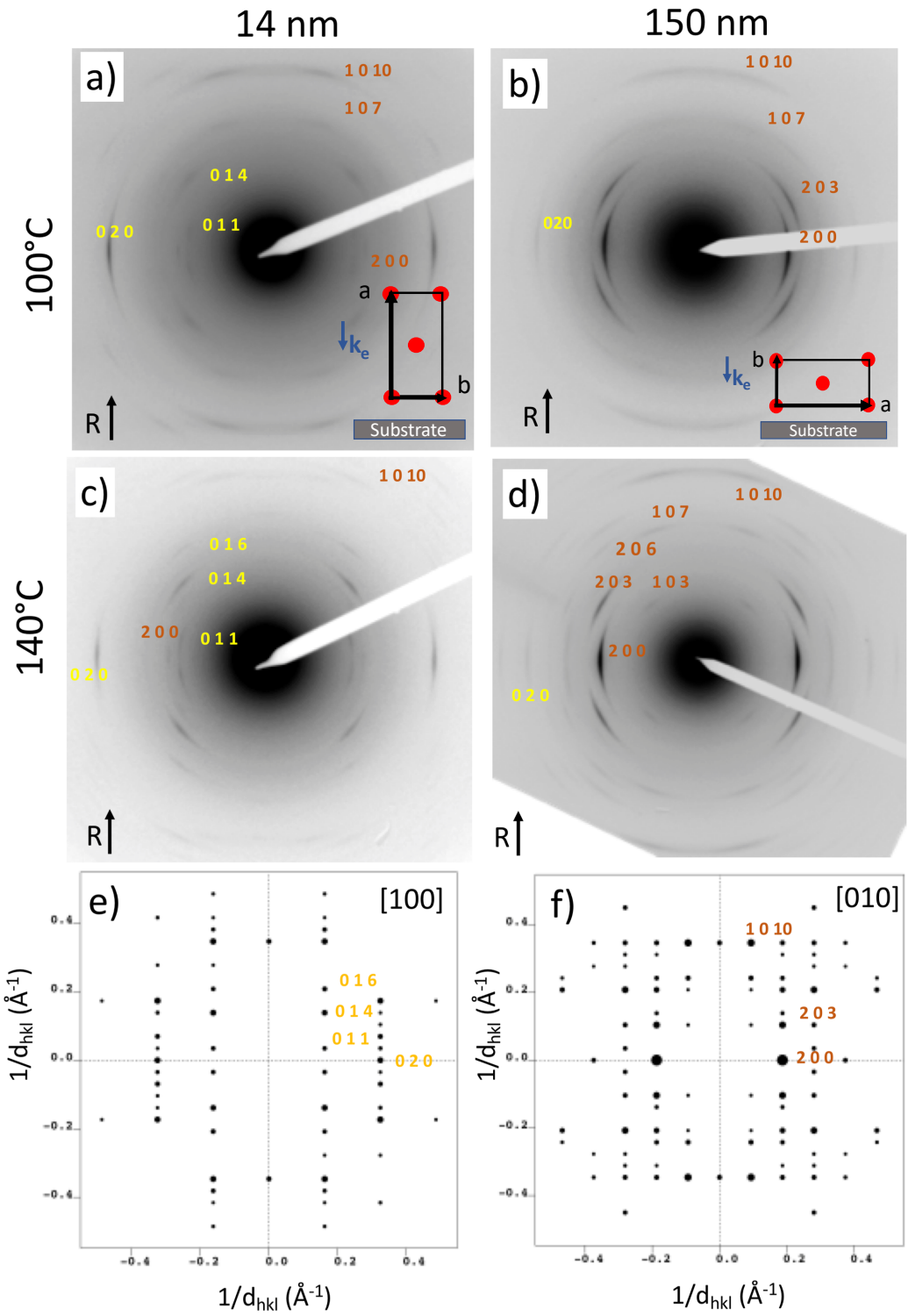

Figure 5. Comparison of the electron diffraction patterns of rubbed PLLA films for two thicknesses (14 nm and 150 nm) and for two rubbing temperatures (T_R=100°C and 140°C). The reflections were indexed using the α structure of PLLA and the yellow and orange colours correspond to the reflections associated with the [100] and [010] contact plane of the PLLA

crystals. The electron diffraction patterns calculated for the two contact planes are depicted in e) and f). The insets in a) and b) show the orientation of the electron beam (k_e) with respect to the lattice of a PLLA with the dominant (100) and (010) contact planes., respectively.

To conclude on the polymorphism of the rubbed PLLA films, we can identify at least three different phases. For T_R=80°C, an oriented mesophase is formed. DSC indicates that this mesophase is metastable and transforms to the α' phase at a temperature in the range 80-100°C and further to the α phase at T=155°C. When the rubbing temperature is in the range 100-120°C, the rubbed films consist of a mixture of oriented α and α' crystals. Finally, for T_R>120°C, the rubbed films consist essentially of the oriented α form. TEM shows also that the orientation of PLLA crystals in the films on glass substrate depend on the film thickness. Increasing film thickness tends to change the dominant contact plane from (100) for 14nm-thick films to (010) for 150nm thick films.

2. Orientation of the PLA stereo-complex.

The high orientation of the PLLA reached by high-T rubbing is an incentive to apply this method to the stereo-complex (SC). Thin SC PLA films can be readily prepared by blending PLLA and PDLA in equal proportions in $CHCl_3$ and preparing SC films by doctor blading. In Figure S5, we show the POM images of the SC PLA films oriented at increasing T_R between 120°C and 200°C. As expected from their higher melting temperature, higher T_R is necessary to observe important birefringence of the SC PLA thin films. In particular, very high orientation is observed for T_R=200°C.

In order to determine the structure of the films after rubbing, DSC was performed on the films oriented at various T_R (Figure 6). The pristine doctor bladed films show two exotherms at 90°C

and 155°C. The first exotherm corresponds to the cold crystallization of PLLA and PDLA. The second exotherm close to 155°C corresponds to the expected melting/recrystallization of α' PLLA and PDLA. The α crystals of PLLA and PDLA subsequently melt at 174°C. The second endotherm at 223°C is due to the melting of SC PLA. Its presence indicates that melting of PLLA and PDLA is followed by a recrystallization in the form of SC crystals.

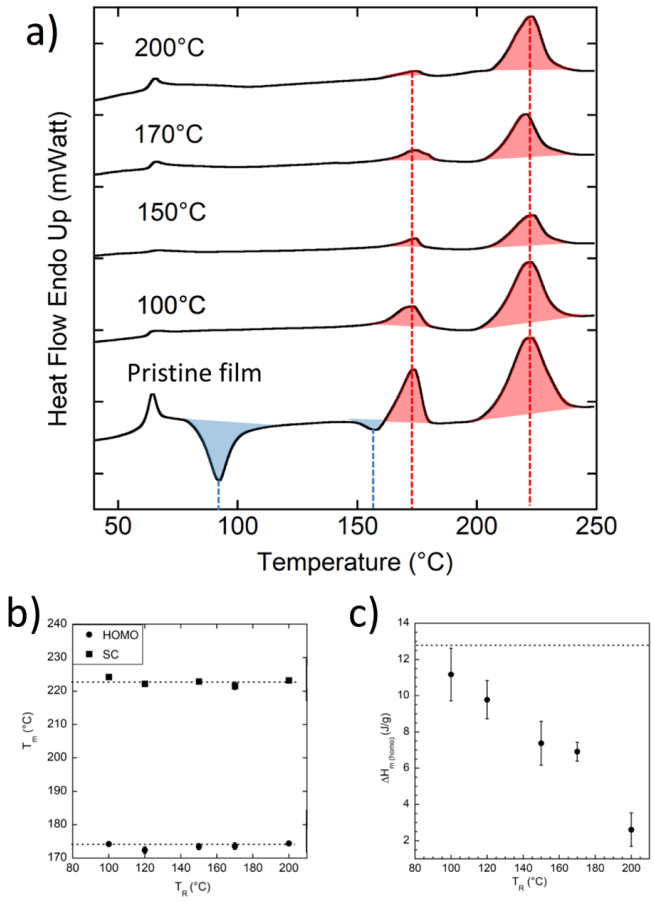

Figure 6. a) Evolution of the first DSC heating cycle in oriented rubbed SC PLA thin films (100nm thickness) as a function of the rubbing temperature. Cold crystallization exotherms are highlighted in blue and melting endotherms in red. b) Melting temperatures of PLLA/PDLA homo-crystals and of the SC PLA. the dotted lines correspond to the melting temperatures in pristine non-rubbed thin films. c) Melting enthalpy of the PLLA/PDLA homo-crystals present in the rubbed thin films as a function of the rubbing temperature.

In the rubbed films, no exotherm observed for PLLA is seen at 90°C and only two exotherms at 173°C and at 223°C are present. The 173°C endotherm is due to the melting of homocrystals of PLLA (PDLA). The apparent melting enthalpy ΔH_m(homo) of this peak continuously decreases with increasing T_R indicating that the amount of homo-crystals of PLLA/PDLA in the thin films decreases with T_R at the expense of crystalline SC PLA.

Further information on the polymorphism of SC PLA films is gained from FTIR spectroscopy. The α, α' and SC PLA structures have characteristic FTIR signatures. [29,30] Figure 7 illustrates two spectral ranges with signatures of the homo-crystals (α/α') and the SC PLA crystals. The 924 cm^{-1} and 908 cm^{-1} bands have been previously ascribed to the 10_3 helical conformation of homocrystals (α and α') and to the 3_1 helical conformation of the chains in the PLA SC crystals, respectively. [29] As seen in Figure 7.a, there is a clear increase of the 908 cm^{-1} band intensity when T_R reaches 200°C indicating a progressively higher proportion of SC PLA crystal. Conversely, the very weak 921 cm^{-1} band associated with the α/α' phases tends to disappear. This is fully consistent with the results drawn from DSC analysis that underline the coexistence of the SC PLA crystalline phase with the homocrystals of PLLA and PDLA in various proportions depending on T_R. A similar effect is seen for the FTIR spectra in the 1240-1320 cm^{-1} range where the 1294 cm^{-1} band of the α'/α phases tends to disappear when T_R increases from 100°C to 200°C whereas the 1306 cm^{-1} band that is characteristic of the SC PLA becomes dominant.[29]

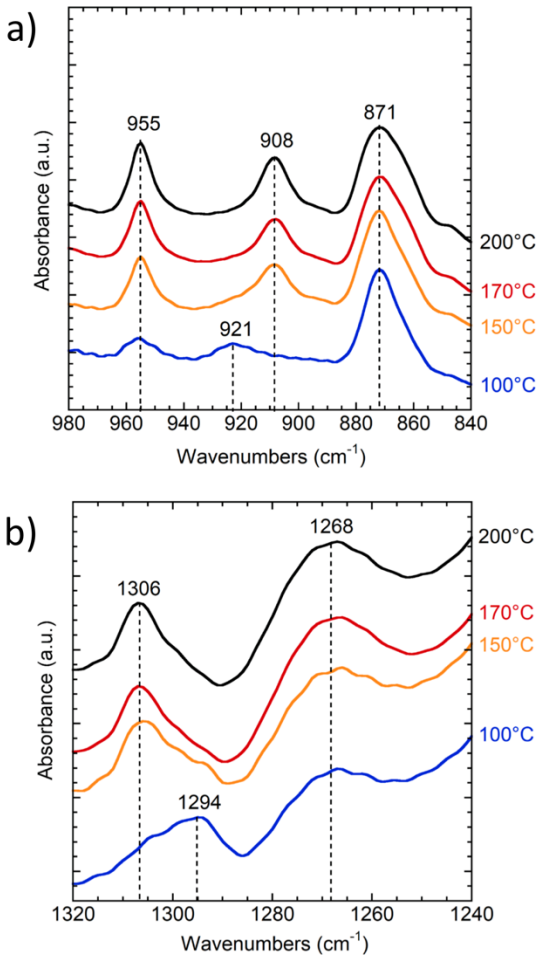

Figure 7. Evolution of the FTIR spectra of oriented thin films of SC PLA thin films (100nm) as a function of the rubbing temperature. For clarity the spectra have been normalized in intensity and shifted along the ordinate axis. The 908 cm^{-1} and 921 cm^{-1} bands are assigned to the coupling of the C-C backbone stretching and the CH_3 rocking mode that depends on the chain conformation (3_1 for 908 cm^{-1} and 10_3 for 921 cm^{-1}).

Finally, the evolution of the SC film structure with T_R was also followed by electron diffraction analysis. Figure 8.a-d show the typical ED patterns for 50nm-thick oriented films obtained by rubbing at different temperatures. The equatorial section profiles of the ED patterns are shown in Figure 8.e. Typical reflections are indexed using the α/α' crystal structure (in black) and the trigonal SC PLA structure (in orange).[8] The ED pattern of the films rubbed at 100°C show

essentially the reflections of α/α' phases without clear evidence of crystalline SC. However, a careful analysis of the equatorial plot profile in 7.d indicates that there are some very weak reflections (1 1 0, 3 0 0 and 2 2 0) that correspond to crystalline SC PLA. This result is surprising as 100°C is very far from the optimal crystallization temperature of SC PLA. At T_R=120°C, the ED pattern shows clear signatures of the SC crystals: the 1 1 0 and 2 2 0 reflections are stronger than for T_R=100°C. Conversely, the intensity of the 2 0 0 and 2 0 3 reflections of the α/α' phases tends clearly to decrease compared to T_R=100°C. For T_R=140°C, the same trend is observed with a progressive increase of the SC PLA reflections whereas the α/α' reflections decrease in intensity. Accordingly, for 100°C≤T_R≤140°C, there is a clear coexistence of the homo-crystals and SC PLA crystals with an increasing proportion of SC crystals. For T_R=200°C, the ED pattern of the SC PLA crystals is "pure" and compares perfectly with the calculated fiber pattern for the SC PLA structure (see Figure 8.f).[11] No reflections of the homocrystals are observed although DSC evidenced some minor traces of PLA homo-crystals (see Figure 6). The lamellar morphology of SC PLA revealed by TEM in Bright Field, has a 21±1 nm periodicity (see Figure S5). Accordingly, rubbing the PLLA/PDLA 1:1 films at 200°C affords almost pure oriented SC films without any remaining α phase of the homopolymers. It is worth mentioning that it is rather difficult to obtain pure oriented SC films in extruded thin films. It is difficult to fabricate extruded SC films due to the rheological properties of the blends. This is why Zhang et al. used asymmetric PLLA and PDLA blends with different M_w to form oriented SC films by hot drawing under appropriate annealing conditions.[29] Similar highly oriented SC but thicker films were prepared by thermal annealing for 10 hr at 200°C of stretched (5 times at 100°C) 1:1 PLLA/PDLA blends cast from chloroform solution.[35] In terms of processing, high-T rubbing might therefore be an interesting approach to reduce annealing times.

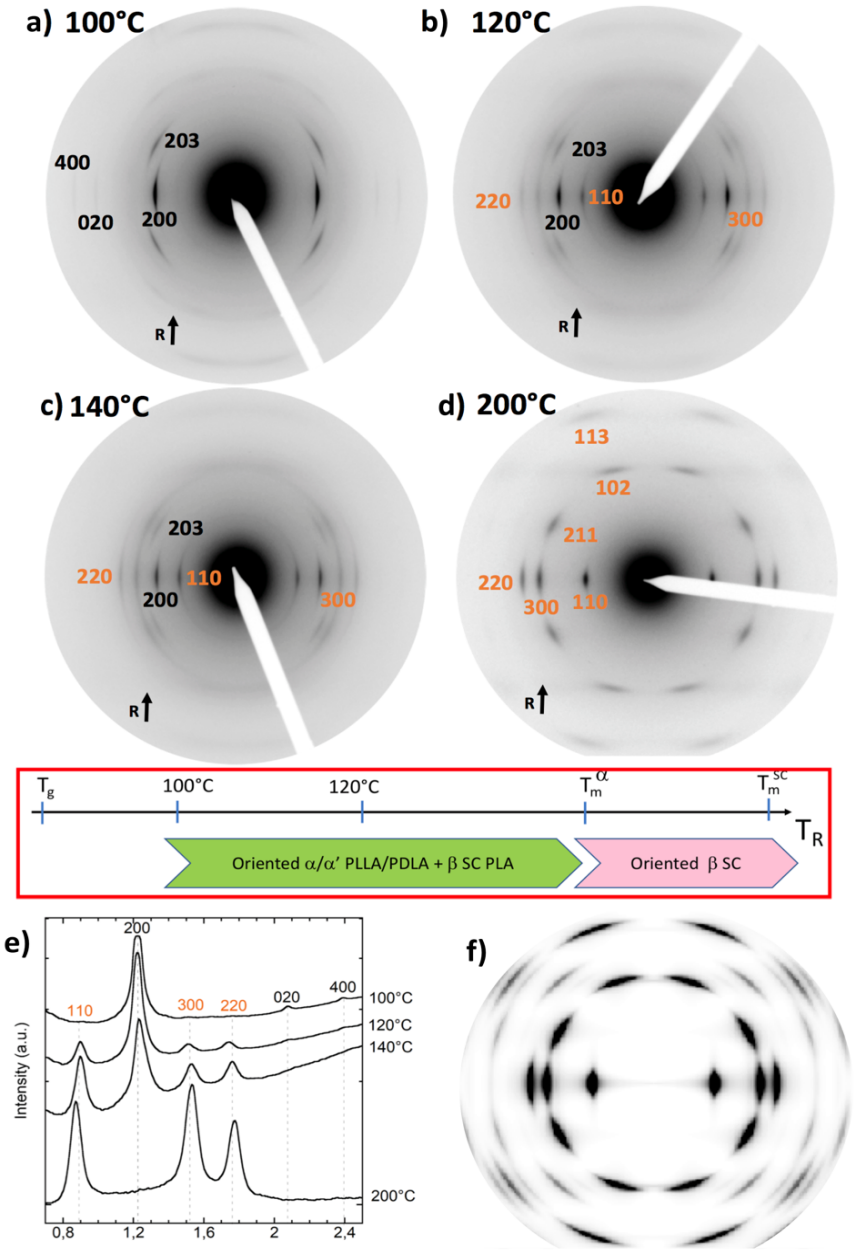

Figure 8: Influence of the rubbing temperature (T_R) on the structure of a stereocomplex film as observed by electron diffraction in Transmission Electron Microscopy (TEM). (a)-(d): Electron diffraction patterns of a stereocomplex thin film (50nm) rubbed at 100°C (a) , 120°C (b), 140°C (c) and 200°C (d). The rubbing direction R is vertical for all patterns. The main reflections of the homo-crystals of PLLA/PDLA are indexed in black and those of the SC PLA in orange (e) : Equatorial section profile of the diffraction patterns versus rubbing temperature. (f) Calculated fiber pattern for the crystalline PLA SC phase.[11]

IV. Conclusion.

High-T rubbing is an interesting and versatile method to prepare highly oriented and crystalline thin films of both PLLA and PLA SC. The temperature at which the films are rubbed is crucial to control the in-plane orientation and the polymorphism of the films. For PLLA, three regimes of T_R are identified. For $T_g \leq T_R < 90°C$, PLLA films consist of an oriented mesophase that undergoes a cold crystallization to the α' phase when annealed at 90-100°C. For $90°C \leq T_R \leq 120°C$, the rubbed PLLA films are composed of a mixture of α and α' phases with a progressive increase of the α phase proportion. Finally, for $T_R \geq 120°C$ the PLLA films are made of α phase with a uniform lamellar morphology. Regardless of polymorphism, increasing T_R leads to an increase in the in-plane orientation of the crystalline domains and a crystallinity of 53% is reached for $T_R = 140°C$. Interestingly, the dominant contact plane of PLLA crystals in rubbed films depends on the films thickness. As for SC PLA films, rubbing at very high temperature (200°C) affords almost pure oriented and crystalline SC PLA films. From the morphology point-of-view, the best aligned α PLLA films prepared at $T_R = 140°C$ and PLA SC for $T_R = 200°C$ show pin holes and are therefore not optimized for applications that require continuous thin films (barrier films, substrates to align molecules, piezoelectric layers). In a forthcoming communication, rubbing at moderate temperature combined with appropriate thermal annealing will be introduced as an effective method to prepare highly crystalline and oriented PLLA films of thickness up to 10 μm.

Acknowledgments.

We thank the TEM platform from ICS for technical support. Support from ANRT through Cifre PhD grant 2018/0723 is acknowledged (MB). Guillaume Rogez (IPCMS, Strasbourg) is acknowledged for giving access to the FTIR spectroscopy laboratory. Mélanie Legros is acknowledged for performing the GPC analysis of the PLLA materials. We thank also

Catherine Saettel for the DSC measurements. We want also to thank Bernard Lotz for a critical reading of the manuscript and fruitful discussions on PLA polymorphism.

Conflict of interest

The authors declare no conflict of interest

References.

(1) L.-T. Lim, R. Auras, M. Rubino, *Progress in Polymer Science* **2008**, *33*, 820.

(2) K. Matsunari, and Y. Kimura *Present Situation and Future Perspectives of Poly(lactic acid).* In: Di Lorenzo, M.; Androsch, R. (eds) Synthesis, Structure and Properties of Poly(Lactic acid). *Advances in Polymer Science*, vol. 279. Springer, Cham. **2017**

(3) M. Vert S. M. Li , G. Spenlehauer and P. Guerin , *J. Mater. Sci. Mater. Med.* **1992**, *3*, 432.

(4) R. M. Rasal, A. V. Janorkar, and D.E. Hirt, *Prog. Polym. Sci.* **2010**, *35*, 338

(5) M. Cocca, M. L. Di Lorenzo, M. Malinconico, and V. Frezza, *Euro. Polym. J.* **2011**, *47*, 1073.

(6) M. L. Di Lorenzo, and R. Androsch, *Polymer International* **2019**, *68*, 320.

(7) S. Saeidlou M. A. Huneault , H. Li C.B. Park *Prog. Polym. Sci.* **2012**, *37*,1657.

(8) B. Lotz, *Crystal Polymorphism and Morphology of Polylactides*, In: Di Lorenzo, M.; Androsch, R. (eds) Synthesis, Structure and Properties of Poly(Lactic acid). *Advances in Polymer Science*, vol. 279. Springer, Cham. **2017**

(9) Y. Ikada, K. Jamshidi, H. Tsuji, S. H. Hyon, *Macromolecules* **1987**, *20*, 904.

(10) H. Tsuji, *Macromolecular Bioscience* **2005**, *5*, 569.

(11) L. Cartier, T. Okihara, Y. Ikada, H. Tsuji, J. Puiggali, and B. Lotz, *Polymer* **2000**, *41*, 8909.

(12) H. Bai, C. Huang, H. Xiu, Q. Zhang, H. Deng, K. Wang, F. Chen, Q. Fu, *Biomacromolecules* **2014**, *15*, 1507.

(13) L. Aliotta, P. Cinelli, M. B. Coltelli, M. C. Righetti, M. Gazzano, A. Lazzeri, *European Polymer Journal* **2017**, *93*, 822.

(14) K. Das, D. Ray, I. Banerjee, N. R. Bandyopadhyay, S. Sengupta, A. K. Mohanty, M. Misra, *Journal of Applied Polymer Science* **2010**, *118*, 143.

(15) A. Guinault, G. H. Menary, C. Courgneau, D. Griffith, V. Ducruet, V. Miri, C. Sollogoub, *AIP Conference Proceedings* **2011**, *1353*, 826.

(16) G. Kokturk, E. Piskin, T. F. Serhatkulu, M. Cakmak, *Polymer Engineering & Science* **2002**, *42*, 1619.

(17) Y. Li, R. Xin, S. Wang, Z. Guo, X. Sun, Z. Ren, H. Li, L. Li, S. Yan, **2021**, *54*, 9124.

(18) J. Petermann, J. M. Schultz, *Colloid and Polymer Science* **1984**, *262*, 217.

(19) J.-F. Ru, S. – G. Yang, D. Zhou, H.-M. Yin, J. Lei, Z.-M. Li, *Macromolecules* **2016**, *49*, 3826.

(20) L. Biniek, N. Leclerc, T. Heiser, R. Bechara, M. Brinkmann, *Macromolecules* **2013**, 46, 4014.

(21) L. Biniek, S. Pouget, D. Djurado, E. Gonthier, K. Tremel, N. Kayunkid, E. Zaborova, N. Crespo-Monteiro, O. Boyron, N. Leclerc, S. Ludwigs, M. Brinkmann, *Macromolecules*. **2014**, 47, 3871.

(22) A. Hamidi-Sakr, L. Biniek, S. Fall, M. Brinkmann, *Adv. Funct. Mater.* **2016**, 26, 408.

(23) M. Brinkmann, S. Pratontep, C. Chaumont, J.-C. Wittmann, *Macromolecules* **2007**, *40*, 9420.

(24) L. Hartmann, D. Djurado, I. Florea, J.-F. Legrand, A. Fiore, P. Reiss, S. Doyle, A. Vorobiev, S. Pouget, C. Chandezon, O. Ersen, M. Brinkmann, *Macromolecules* **2013**, *46*, 6177.

(25) J. Zhu, L. Jia, R. Huang, *Journal of Materials Science: Materials in Electronics* **2017**, *28*, 12080.

(26) S. J. Lee, A. P. Arun, K. J. Kim, *Materials Letters* **2015**, *148*, 58.

(27) J. Hu, L.-L. Han, T.-P. Zhang, Y. X. Duan and J.-M. Zhang, *Chinese J. Polym. Sci.* **2019**, 37, 253.

(28) G. Stoclet, R. Seguela, J. M. Lefebvre, S. Elkoun, C. Vanmansart, *Macromolecules* **2010**, *43* (3), 1488.

(29) J. Zhang, K. Tashiro, H. Tsuji, A. J. Domb, *Macromolecules* **2008**, *41*, 1352.

(30) P. Pan, J. Yang, G. Shan, Y. Bao, Z. Weng, A. Cao, K. Yazawa, Y. Inoue, *Macromolecules* **2012**, *45*, 189.

(31) D. Sawai, K. Takahashi, A. Sasashige, T. Kanamoto, S.-H. Hyon, *Macromolecules* **2003**, *36*, 3601.

(32) J.-J. Hermans, P.-H. Hermans, D. Vermaas, and A. Weidinger, *Rec. Trav. Chim.* **1946**, 65, 427.

(33) F. Mai, W. Tu, E. Bilotti, T. Peijs, *Fibers* **2015**, *3*, 523.

(34) C. Vergnat, V. Landais, J. Combet, A. Vorobiev, O. Konovalov, J.-F. Legrand, M. Brinkmann, *Org. Elect.* **2012**, *13*, 1594.

(35) K. Tashiro, N. Kouno, H. Wang, H. Tsuji, *Macromolecules* **2017**, *50*, 8048.